International Journal of Applied Pharmaceutics

ISSN- 0975-7058 Vol 16, Issue 2, 2024

Original Article

DEVELOPMENT AND EVALUATION OF NANOBIOCOMPOSITE TOPICAL FORMULATION

MANISHA JADAV[1*], VANDANA PATEL[2], LALIT LATA JHA[1]

[1*]School of Pharmacy, Parul University, P. O. Limda, Ta. Waghodia, Vadodra-391760, Gujarat, India. [2]Krishna School of Pharmacy and Research, Varnama, Vadodara-391240, Gujarat, India

*Corresponding author: Manisha Jadav; *Email: manisha.jadav121112@paruluniversity.ac.in

Received: 05 Oct 2023, Revised and Accepted: 29 Jan 2024

ABSTRACT

Objective: The proposed research involving transferosomes within a hydrogel matrix offers a promising approach for enhanced wound healing. This system aims to facilitate the dermal delivery of nanosized curcumin while incorporating Ascorbic acid and Salicylic acid. The integration of these components holds the potential for advancing chronic wound therapy.

Methods: Curcumin transferosomes were formulated by the lipid thin film hydration method and further optimization was carried out using 3^2 full factorial design. The transferosome formulation, prepared using phospholipon 90G, involved selecting specific variables: the quantity of edge activator and sonication duration as independent factors, while the optimization process considered particle size and entrapment efficiency as dependent variables. Following the optimization of the transferosomes, a hydrogel formulation was developed using the central composite design approach.

Results: Optimized transferosome (Batch F8) showed 87.75±3.74 nm (nanometer) particle size and 91.18±2.71% entrapment efficiency. Hydrogel was formulated by Central composite design, selecting pH and spreadability as dependent factors, to which was added curcumin transferosomes, Ascorbic acid and Salicylic acid. The data was analyzed using Stat-ease Design-Expert v7.0.0 software. The optimized batch F3 showed a pH of 6.84, spreadability of 12.89 gm. cm/sec and Curcumin release of 87.47%. Drug release from nanobiocomposite hydrogel was evaluated using the *in vitro* study of the formulation. The various kinetic models were applied to *in vitro* release data for the prediction of the drug release kinetic mechanism. The release constants were calculated from the slope of appropriate plots, and the regression coefficient (R^2) was determined. It was found that the *in vitro* drug release of the formulation was best explained by Higuchi as the plots show the highest linearity. The regression coefficient (R^2) was found to be 0.907, 0.9266 and 0.9536 for Ascorbic acid, Salicylic acid and Curcumin, respectively.

Conclusion: The nanobiocomposite topical formulation was thus prepared, tested and for skin irritancy study. There is no noticeable signs of erythema, edema, or inflammation were observed on the skin. These results indicate that the developed transdermal formulation does not cause skin irritation and can be considered non-irritating.

Keywords: Curcumin, Hydrogel, Nanobiocomposite, Transferosomes

DOI: https://dx.doi.org/10.22159/ijap.2024v16i2.49561 Journal homepage: https://innovareacademics.in/journals/index.php/ijap

INTRODUCTION

Chronic wounds represent a significant burden on healthcare systems, necessitating the development of advanced wound-healing approaches. This study focuses on the formulation of a transferosome-in-hydrogel system for the dermal delivery of nanosized curcumin, along with ascorbic acid and salicylic acid, to enhance chronic wound therapy. A wound is characterized by the disruption of epithelial cells, either with or without damage to the underlying cell layers. The healing of wounds involves a complex interplay of biochemical processes as a natural response to tissue damage. These processes can be categorized into four stages: hemostasis, inflammation, proliferation, and maturation [1]. Curcumin, chemically known as (1E, 6E)-1,7-bis(4-hydroxy-3-methoxyphenyl) hepta-1,6-diene-3,5-dione, has gained attention for its various therapeutic properties. Curcumin's array of therapeutic effects has been widely recognized, encompassing anti-inflammatory, antibacterial, wound healing, anti-cancer, antioxidant, hyperlipidemic, and hepatoprotective attributes [2]. Ascorbic acid, also known as Vitamin C, is a natural water-soluble vitamin. It plays a vital role in collagen synthesis, essential for the formation of fibrous tissue, teeth, bones, connective tissue, skin, and capillaries. Ascorbic acid acts as a potent reducing and antioxidant agent, contributing to the body's defense against bacterial infections and facilitating detoxification processes. Unlike many other animals, humans cannot synthesize or store and it must be obtained through dietary sources such as citrus fruits and vegetables [3]. Transferosomes are optimized lipid-based supramolecular aggregates that possess high deformability, allowing them to penetrate mammalian skin effectively [4]. These lipid vesicles incorporate an edge activator, such as Span 80 or Tween 80, and consist of an inner aqueous phase enclosed by a lipid bilayer [5]. Transferosomes, resembling cell vesicles involved in exocytosis, hold promise as carrier systems for regulated and potentially targeted drug delivery [6].

In this research, we propose the development and optimization of a transferosome-in-hydrogel system for advanced wound healing [7-9]. The system aims to deliver nanosized curcumin, along with ascorbic acid and salicylic acid, to enhance the therapeutic outcomes of chronic wound treatment [10-13]. The formulation and optimization of the transferosomes and hydrogel will be carried out; key parameters such as particle size, spreadability, pH, and entrapment efficiency [14-17]. The effectiveness and safety of the resultant nano biocomposite topical formulation will be thoroughly assessed via both *in vitro* and *in vivo* investigations [18-20]. To assess the stability of the formulation, a comprehensive stability study was conducted under accelerated and long-term storage conditions. The nanobiocomposite topical formulation was subjected to temperature and humidity variations to evaluate its physical and chemical stability over time. Particle size, drug content, entrapment efficiency and drug release profile were monitored at predetermined intervals to assess any changes in the formulation's properties. The nanocomposite topical formulation thus prepared will be tested for skin irritancy study using albino Wistar rats [21, 22]. Overall, the utilization of curcumin, ascorbic acid, salicylic acid, and transferosomes in a hydrogel system holds great potential for promoting wound healing and improving patient outcomes [23, 24].

MATERIALS AND METHODS

Curcumin and Ascorbic acid were procured from Himedia, Mumbai. Phospholipon 90G was purchased from Lipoid, Germany. Span 80 was procured from Chemdyes, Vadodara. Chloroform, disodium hydrogen phosphate, and potassium dihydrogen phosphate were obtained from S D Fine Chemical Limited, Vadodara. Carbopol 934 was purchased from a supplier in Maharashtra. Propylene glycol and

Methyl paraben were purchased from Chemdyes, Rajkot. Honey was obtained from Dabur India, Kolkata. Salicylic acid was obtained from Finar Limited, Ahmedabad. Glycerol and Triethanolamine were purchased from Oxford Lab Fine Chem Ltd, Maharashtra.

Preparation of transferosome

Two different lipids (Phospholipon 90G and Phospholipon 90H) were used for screening of lipids. Screening of phospholipids was conducted based on the percentage entrapment efficiency and vesicle size, as indicated in table 1. Preparation of curcumin transferosomes was carried out by using selected Phospholipon 90G lipid and applying 3^2Full factorial design. Process parameters (table 2) for the preparation of transferosomes were optimized. Transferosomes were prepared using the thin film hydration technique, with chloroform employed as the solvent. Take phospholipid and edge activator and curcumin in a round bottom flask, add chloroform, and dissolve it. Evaporate Excessive solvent until a thin film forms and then hydrate it with phosphate buffer 7.4 and gently shake for 15 min. Yellowish-colored curcumin transferosome suspension is formed. Variable selected for Formulation prepared by using Phospholipon 90G i.e. the amount of edge activator [milligram (mg)] and sonication time (min) were selected as independent variables, while particle size [nanometer (nm)] and entrapment efficiency (%) were considered as dependent variables in the optimization process. Through an extensive literature survey, various ratios were identified and used to formulate different batches. The optimization study was performed using a 3^2 full factorial design. Among the assessed batches, Batch F8 displayed the smallest particle size and the greatest entrapment efficiency.

Characterization of curcumin loaded-transferosomes

The transferosomes loaded with curcumin underwent comprehensive characterization. To achieve this, a one-milliliter portion of the transferosomal suspension was diluted with 10 milliliters of double-distilled water [17]. The dimensions of the vesicles, their distribution, and the zeta potential were assessed using a laser scattering particle size analyzer depicted in fig. 1 (Malvern zeta sizer, MAL1065515).

Drug entrapment efficiency and its calculation

The drug entrapment efficiency of the transferosomal suspensions was ascertained through ultracentrifugation at 14,000 [Rotation per minute (rpm)] and 10 °C for 30 min. After centrifugation, 1 milliliter of the resulting supernatant was mixed with 9 milliliters of phosphate saline buffer (pH 7.4). [18, 24] Subsequently, the diluted solution's absorbance was gauged at a wavelength of 254 nm using a UV-Vis spectrophotometer (Shimadzu-1900i).

Drug entrapment efficiency was then calculated using the formula:

$$\text{Entrapment Efficiency (\%)} = (\text{Total drug amount} - \text{Amount in supernatant})/(\text{Total drug amount}) \times 100$$

Preparation of hydrogel

Carbopol concentration (%) and stirrer speed (rpm) were selected as independent variables for formulation preparation using Carbopol 934. pH, spreadability, and curcumin release were taken as dependent variables. Weigh Carbopol 934 and soak it in 10 milliliters water for 24 h. Add propylene glycol, honey, methyl paraben, and glycerol along with the addition of curcumin Transferosomal solution, ascorbic acid, and salicylic acid. The above dispersion is neutralized with triethanolamine to adjust pH 6.8. Stirred above Dispersion for 15-20 min using a remi stirrer.

pH analysis

The pH of hydrogel was analyzed using a digital pH meter, with the glass electrode fully submerged in the gel to ensure complete coverage. This pH assessment was performed three times, and the resulting average of these triple readings was documented.

Viscosity measurement

The viscosity of the hydrogel sample was assessed utilizing the labman scientific viscometer. This evaluation involved utilizing spindle L2, set to a rotational speed of 120 rpm, and a controlled temperature of 28 °C. A proper quantity of the hydrogel was placed into a suitable wide-mouth receptacle, ensuring the spindle of the viscometer could be fully immersed. Before measurement, the hydrogel samples were allowed to settle for 30 min at a consistent temperature of 28 °C±1 °C.

Spreadability

Nanobiocomposite hydrogel formulation was equilibrate to the room temperature. Place a measured amount of the hydrogel on a glass slide. Gently and evenly spread the hydrogel to form a thin and uniform layer. Create a sandwich-like structure by placing another glass slide on top. Hold the two glass slides firmly and slide them apart horizontally with a constant force. Measure the distance the hydrogel spreads in a specific time frame i.e. 30 seconds. Repeat the procedure for multiple portions of the hydrogel and calculate the average spreadability distance. The spreadability is then calculated using a formula

$$[\text{Spreadability}\left(\text{gm}\cdot\frac{\text{cm}}{\text{sec}}\right) = \text{Mass of the hydrogel spread(gm)} \times \text{Distance spread in 30 seconds(cm)}$$

that considers the mass of the hydrogel and the distance it spreads in the given time.

Curcumin release

The receptor medium employed was a pH 7.4 phosphate buffer solution. The experimental setup involved the utilization of a Franz diffusion cell, with a specially chosen parchment paper acting as the separation membrane. The hydrogel sample, containing the curcumin drug formulation, was delicately applied onto the parchment paper and securely positioned between the donor and receptor compartments of the diffusion cell. To establish a consistent milieu, the receptor compartment was filled with 25 ml of phosphate buffer (pH 7.4) solution. Temperature control was achieved through the incorporation of a water jacket, maintaining a constant temperature of 37 °C±0.5 °C. The implementation of magnetic stirring further guaranteed the uniformity of the medium. After 24 h, aliquots of 1 ml were meticulously collected from the receptor medium. Immediate replenishment with an equivalent volume of fresh buffer solution was carried out after each withdrawal to sustain the sink condition. The analysis of the released drug concentrations entailed the measurement of absorbance for curcumin in the withdrawn samples, accomplished at 254 nm utilizing high-performance liquid chromatography (HPLC). The concentrations were subsequently quantified utilizing the established calibration curves for each compound, including all thirteen batches.

***In vitro* diffusion experiments**

In this study, we used a pH 7.4 phosphate buffer solution as the receptor medium. A Franz diffusion cell was employed, and parchment paper served as the membrane. The hydrogel sample containing the drug formulation was applied onto the parchment paper and positioned securely between the donor and receptor compartments of the diffusion cell. The receptor compartment was filled with 25 ml phosphate buffer (pH 7.4). To maintain a constant temperature of 37 °C±0.5 °C, a water jacket was utilized, and magnetic stirring ensured homogeneity of the medium.

At specific time intervals (0.5, 1, 2, 4, 6, 8, 12, and 24 h), we collected 1 ml sample of the receptor medium. After withdrawal, each sample was immediately replaced with an equal volume of fresh buffer solution to maintain the sink condition. To analyze the released drug concentrations, we measured the absorbance of curcumin, ascorbic acid, and salicylic acid in the withdrawn samples at 254 nm using high-performance liquid chromatography. The concentrations were determined using calibration curves for each compound.

Study of drug release and kinetic mechanism

The drug release from the nanobiocomposite hydrogel was evaluated in an in vitro study conducted using a Franz diffusion cell [25]. The receptor compartment of the diffusion cell was filled with phosphate buffer (pH 7.4). The dissolution medium was maintained at a temperature of 37 °C±0.5 °C to simulate physiological condition.

To ascertain the most appropriate release mechanism describing the

drug release pattern, the in vitro release data were subjected to fitting with various mathematical models, including the first-order model (ln Qt = ln Q0+K1t), zero-order model (Qt = Q0+K0t), Korsmeyer-Peppas model (Qt/Q8 = Ktn) and Higuchi model (Qt = KH t1/2). To compute the model parameters and evaluate the fit quality, regression analysis was conducted on the data using the statistical function within MS Excel.

In vivo study (Skin irritancy study)

To assess the potential skin reaction of the formulation, an in vivo skin irritancy study was carried out on Wistar rats. Animals sourced from Sunpharma Advanced Research Centre (SPARC) Tandalja (69/PO/Rcbis/Rcl/99/CPCSEA) under Protocol No: PIPH 05/23 were housed in polypropylene rat cages (three animals per cage) using corn cob or rice husk as bedding material, and they had ad libitum access to laboratory rat pellet feed and pure drinking water. The abdominal region of the rats, which had been shaved approximately 24 h before the study, was used for the application of the test formulation and a standard irritant solution of formalin (0.8% v/v). Care was taken to prevent any skin abrasion during the application process. The animals were observed at specific intervals: 60 min post-drug removal, as well as at 24, 48, and 72 h. Signs of erythema (redness) and edema (swelling) were examined during these observation periods. As a control, an adjacent untreated skin area on each animal was considered. The evaluation of skin irritation employed a scoring scale, beginning with the initial assessment of one animal right after drug application. Dermal reactions were graded and documented based on predefined criteria. In cases where any skin damage occurred and couldn't be categorized as irritation or corrosion by the 72 h mark, additional observations might have been extended until 14 d to ascertain the potential reversibility of effects.

Stability study

The stability study of the drug-loaded hydrogel was conducted in accordance with the International Council for Harmonisation (ICH) guidelines Q1A (R2). This comprehensive study encompassed the exposure of the hydrogel to distinct storage environments: ambient conditions characterized by room temperature (25 °C±2 °C/60%±5% RH), as well as an accelerated environment at elevated temperature (40 °C±2 °C/75%±5% RH) over a period of three months. The assessment of the hydrogel's stability involved a multifaceted approach. The parameters under scrutiny encompassed alterations in physical appearance, notably changes in color, alongside an investigation into drug content and pH levels. These attributes were subjected to a thorough evaluation, leading to a comprehensive interpretation of the results to discern the hydrogel stability profile.

RESULTS AND DISCUSSION

Physicochemical analysis

Physicochemical analysis of optimized formulation revealed no evidence of interaction between the drugs and polymer [26]. This suggests compatibility between the drugs and the polymer used, which is crucial for ensuring the stability and effectiveness of the formulation. This result supports the feasibility of the formulation in terms of its chemical integrity.

Phospholipid screening

From the screening study of Phospholipids, Phospholipon 90G has good entrapment efficiency and vesicle size as shown in table 1. This finding is essential as it suggests that this particular phospholipid could be a promising component for the formulation, contributing to efficient drug entrapment within vesicles while maintaining an optimal size for drug delivery [27].

Optimal conditions for transferosome preparation

The identified optimal conditions-550 °C temperature, 500 mm Hg pressure, and 80 rpm rotational speed- signify crucial parameters for preparing transferosomes. These conditions likely promote the formation of transferosomes with desirable characteristics, such as stability, size uniformity, and drug encapsulation efficiency.

Film formation and hydration timing

The timeframes provided in table 2 (50-60 min for film formation and one hour for hydration) are significant as they offer insights into the manufacturing process of the transferosomes. The formation of a stable film within this timeframe suggests a controlled and reproducible process, while the subsequent hydration duration is crucial for ensuring the successful formation of transferosomes [28].

Table 1: Screening of phospholipids based on % entrapment efficiency and vesicle size

	Phospholipon 90G	Phospholipon 90H
Lipid	850 mg	850 mg
Drug (Curcumin)	30 mg	30 mg
Chloroform	10 ml	10 ml
Edge activator (Span 80)	150 mg	150 mg
% Encapsulation Efficiency*	89.27±2.48	72.56±5.8
Vesicle size (nm)*	79.24±3.71	120.23±4.56

Data represents mean±SD (n=3)

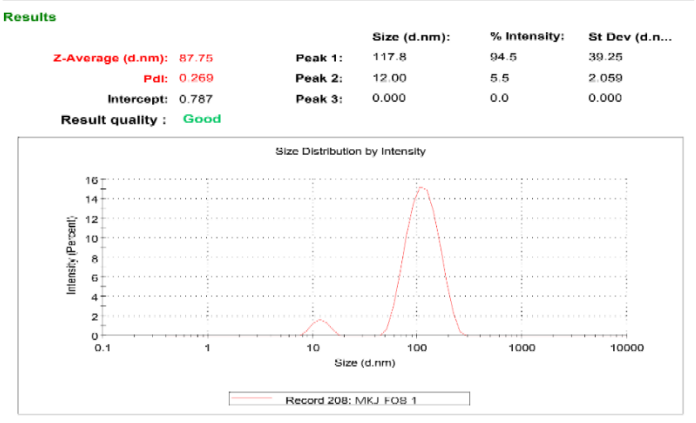

Fig. 1: Particle size graph of curcumin transferosomes by zeta sizer, the findings regarding Batch F8 seem pivotal

Table 2: Optimization of process parameters

X1: Temperature (°C)	X2: Pressure (mm Hg)	X3: Rotation (rpm)g	X4: Time of making film	X5: Time for hydration	Y: Consistency of film
45	300	50	2 h	1.8 h	Thick
50	400	60	1.5 h	1 h	Slightly thin
55	500	80	50-60 min	1 h	Thin

Table 3: Curcumin transferosome optimization by 3^2 full factorial design

Batch	Variables in coded form		Variables in actual form		Response variables*	
	X1: Amount of edge activator	X2: Sonication time	X1: Amount of edge activator (mg)	X2: Sonication time (min)	Particle size (nm)	Entrapment efficiency (%)
F1	-1	-1	100	10	79.02±2.84	45.01±1.85
F2	0	-1	150	10	107.01±3.12	74.09±5.25
F3	+1	-1	200	10	156.19±2.15	65.91±3.49
F4	-1	0	100	15	67.9±3.47	52.18±1.87
F5	0	0	150	15	96.02±4.89	81.91±2.46
F6	+1	0	200	15	129.93±1.28	69.01±3.18
F7	-1	+1	100	20	59.12±2.78	60.05±3.42
F8	0	+1	150	20	87.75±3.74	91.18±2.71
F9	+1	+1	200	20	113.09±2.89	71.09±3.61
F10	0	0	150	15	93.12±5.67	78.91±4.58
F11	0	0	150	15	94.02±2.87	82.12±2.96

Data represents mean±SD (n=3)

Batch F8's superiority

Out of the batches investigated for optimization, Batch F8 displayed the most compact particle size and the greatest entrapment efficiency. These traits are crucial in drug delivery systems, as a smaller particle size often correlates with better drug absorption and higher entrapment efficiency ensures more of the drug is encapsulated within the delivery system.

Optimal formulation parameters

The detailed analysis indicates that the formulation F8, specifically formulated with 150 mg of the edge activator and subjected to 20 min of sonication, demonstrated the most favorable outcomes across all parameters listed in table 3. This result underscores the importance of these specific formulation parameters in achieving the desired characteristics in the transferosomes.

Significant influence of independent factors

Furthermore, the data reveals that both independent factors studied i.e., the amount of edge activator (X1) and sonication time (X2)-have a significant impact on the dependent variables, which are the characteristics of the transferosomes [29]. This emphasizes the critical role that these factors play in determining the quality and properties of the final formulation.

Considering these results alongside existing literature on transferosomes and formulation optimization can help reinforce the significance and novelty of these findings within the broader scientific community [30]. Additionally, discussing the potential mechanisms behind the influence of edge activator quantity and sonication duration on the transferosome characteristics could provide deeper insights into the formulation process.

Table 4: Summary of analysis of variance (ANOVA) for response parameters by 3^2 Full factorial design of curcumin transferosomes

Source	Sum of squares	Degree of freedom	Mean square	F value	P value
Particle size					
Model	7605.87	5	1521.17	146.71	0.0001
Residual	51.84	5	10.37	-	-
Corrected Total	7657.71	10	-	-	-
Entrapment efficiency					
Model	1868.37	5	373.67	75.22	0.0001
Residual	24.84	5	4.97	-	-
Corrected Total	1893.21	10	-	-	-

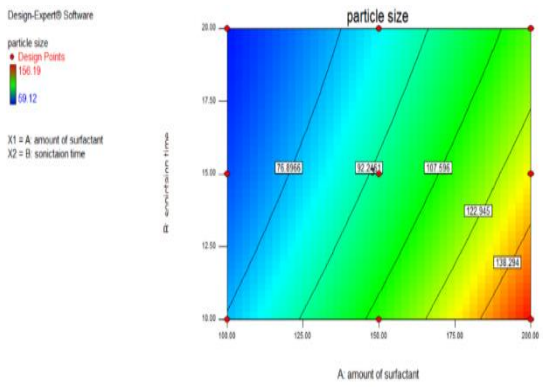

Fig. 2: Contour plot of particle size

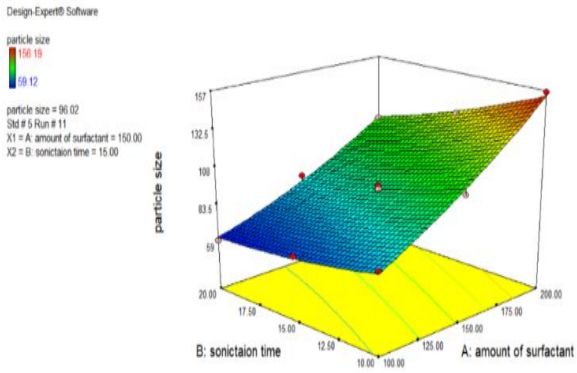

Fig. 3: Response surface plot of particle size

Effect of factors on particle size

Fig. 2 illustrates the response surface plot, which highlights the optimal region of the formulation concerning particle size. The blue region in both the response plot and contour plot (fig. 2 and 3) represents the optimized area where the particle size is minimized. The model's coefficient of determination (R^2) was calculated to be 0.9521, indicating the significance of the model. A value close to 1 suggests that the model explains a significant portion of the variability in the data, strengthening its predictive power.

The polynomial equation for particle size was reduced as follows:

$$\text{Particle size} = +94.31 + 32.20 * A - 13.85 * B + 4.73A\text{^}2 + 2.76 * B\text{^}2$$

This equation reveals the impact of the independent variables on the response, i.e., particle size.

Edge activator quantity

Positive Effect: The positive coefficient suggests that an increase in the amount of edge activator leads to a larger particle size. This indicates that higher quantities of the edge activator component in the formulation tend to result in larger particles. It is important to balance the quantity of edge activator to achieve the desired particle size without compromising other essential characteristics of the transferosomes.

Sonication time

Negative Effect: The negative coefficient indicates that an increase in sonication time results in a gradual decrease in particle size. Longer sonication times appear to contribute to smaller particle sizes, likely due to enhanced dispersion and breakdown of larger aggregates or particles during the sonication process. This suggests that optimizing sonication duration could play a pivotal role in achieving smaller and more uniform particle sizes in the formulation.

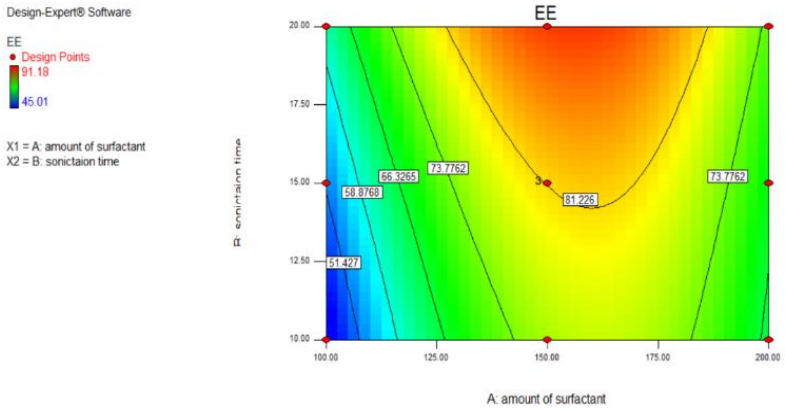

Fig. 4: Contour plot of entrapment efficiency

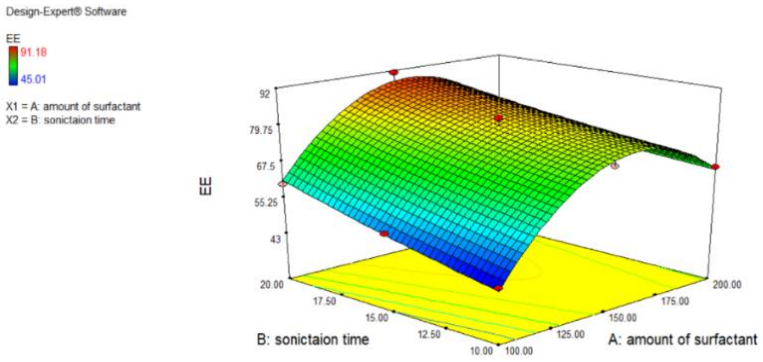

Fig. 5: Response surface plot of entrapment efficiency

Effect of factors on entrapment efficiency

The emphasis on achieving maximum entrapment efficiency for an effective formulation is crucial for ensuring optimal drug delivery. The response surface plot (fig. 5) was interpreted in details. The identification of the orange area in the response surface plot highlights the region where maximum entrapment efficiency is achieved. This area is vital as it signifies the optimal conditions or combination of factors that result in the highest entrapment efficiency within the experimental range.

The R^2 value of 0.9371 indicates that the model used to predict entrapment efficiency is highly significant and accounts for a substantial portion of the variability in the data. This strengthens the reliability of the model in predicting entrapment efficiency based on the formulated equation.

Reduced polynomial equation of entrapment efficiency is given below

$$\text{Entrapment efficiency} = +81.35 + 8.13 * A + 6.22 * B\ 21.30\ A\text{^}2 + 0.74\ B\text{^}2$$

The equation portrays the impact of independent variables on the response, specifically entrapment efficiency.

Quantity of surfactant

Positive effect: The positive coefficient associated with the quantity of surfactant suggests that increasing the amount of surfactant in the formulation positively impacts entrapment efficiency. This indicates that higher quantities of surfactant contribute to increased entrapment of the drug within the transferosomes. It is essential to maintain an amount, ensuring an optimal amount of surfactant for efficient drug encapsulation without compromising other aspects of the formulation.

Sonication time

Positive effect: Similar to the quantity of surfactant, the positive coefficient for sonication time indicates that longer durations of sonication positively influence entrapment efficiency. Increased sonication time likely facilitates better dispersion and encapsulation of the drug within the transferosomes, leading to higher entrapment efficiency. Optimizing sonication duration is crucial for maximizing drug entrapment while maintaining the stability and integrity of the formulation.

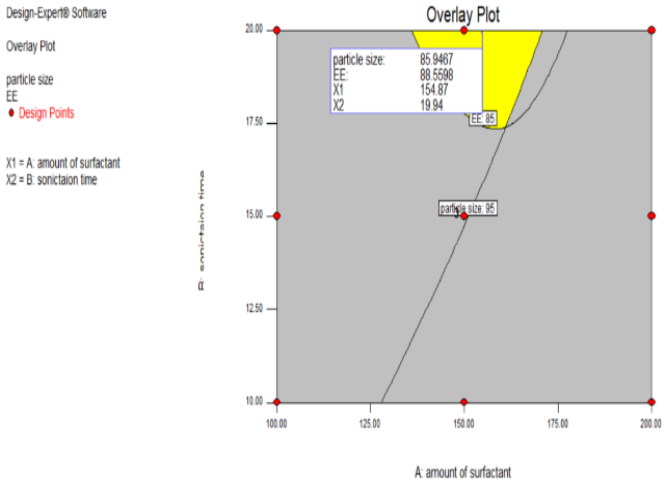

Fig. 6: Overlay plot of particle size and entrapment efficiency

Validation of experimental design

The validation process involving the checkpoint batch (C1 batch) is crucial for confirming the reliability and accuracy of the experimental design used for optimization. Comparing the actual values of the check point batch with the predicted values from the experimental design, as shown in fig. 6, provides insights into the precision and effectiveness of the model [31].

In this example

Predicted Values (from Experimental Design): Amount of edge activator is predicted as 150 mg and Sonication Time is predicted as 20 min

Actual Values (from Check Point Batch-C1 Batch): Amount of Edge Activator is measured as 154.87 mg and sonication time is measured as 19.94 min

Observations

The predicted values and the actual values for the checkpoint batch are very close, indicating a high level of accuracy in the experimental design and the predictive model.

The slight deviation between the predicted and actual values (e. g., 154.87 mg vs. predicted 150 mg for edge activator and 19.94 min vs. predicted 20 min for sonication time) might be within an acceptable range of experimental variability.

Table 5: Comparison of the result of performed checkpoint batch (C1 batch) with actual checkpoint batch (C2 batch) and optimized batch (F3 batch)

	Y1: Particle size (nm)	Y2: Entrapment efficiency (%)
Performed Check point batch (C1 batch)	83.9+1.26	90.55+1.05
Actual check point batch (C2 batch)	85.94	88.55
Optimized batch (F8 batch)	87.75+3.74	91.18+2.71

Data represents mean±SD (n=3)

The analysis demonstrated in table 5, that there were no significant differences between the actual and predicted values for responses Y1 and Y2. This close resemblance between the experimental and predicted responses indicated the robustness of the prediction. As a result, Batch F8 was selected as the optimized transferosome formulation.

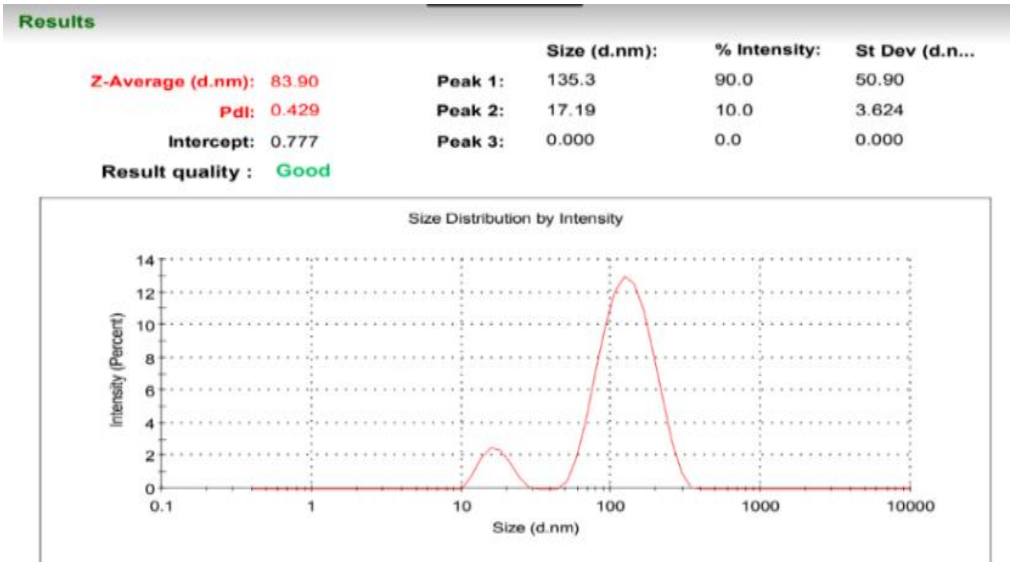

Fig. 7: Particle size graph of performed check point batch

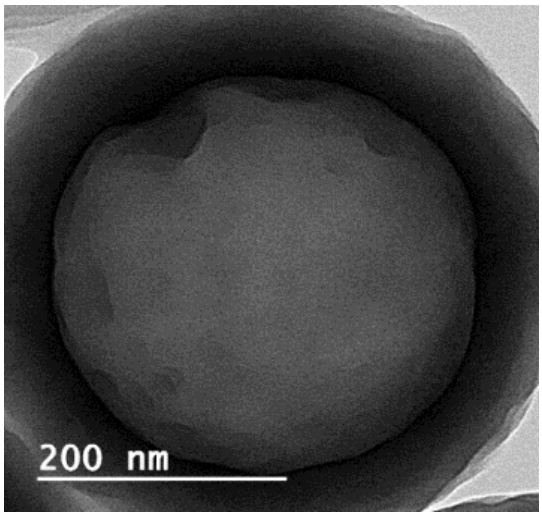

Fig. 8: Transmission electron microscopy (TEM) analysis of curcumin transferosomes

Table 6: Screening of polymer for preparation of gel

Parameters	Carbopol 640	Carbopol 934	Carbopol 971
Appearance	Translucent	Translucent	Translucent
color	Faint Yellow	Faint Yellow	Faint Yellow
Feel on application	Smooth	Smooth	Less Smooth
Viscosity (cP)	3440	4256	3784
Homogeneity	Slightly Homogenous	Homogenous	Homogenous

Table 7: Optimized formula for gel preparation

Ingredients	Quantity
Curcumin	2%
Ascorbic Acid	1%
Salicylic Acid	1%
Propylene glycol	10 %
Glycerol	30 %
Honey	1 %
Carbopol 934	0.5%
Methyl Paraben	0.1%
Triethanolamine	Q. s.
Water	Q. s.

Table 8: Formulation (Hydrogel) optimization by central composite design

Batch	Variables in coded form		Variables in actual form		Response variables		
	X1: carbopol conc	X2: stirrer speed	X1: carbopol conc	X2: stirrer speed	pH	Spreadability (gm·cm/sec)	Curcumin release (%)
F1	-1	-1	1	400	6.81	11.12	88.44
F2	1	-1	1.5	400	7.16	11.57	87.04
F3	**-1**	**1**	**1**	**800**	**6.84**	**12.89**	**87.47**
F4	1	1	1.5	800	7.16	10.99	86.98
F5	-1.414	0	0.90	600	6.75	12.78	88.40
F6	1.414	0	1.60	600	7.2	11.45	86.47
F7	0	-1.414	1.25	317.16	7.16	11.23	87.73
F8	0	1.414	1.25	882.84	7.13	11.54	88.41
F9	0	0	1.25	600	7.09	10.86	87.72
F10	0	0	1.25	600	7.08	10.83	88.80
F11	0	0	1.25	600	7.10	10.89	88.21
F12	0	0	1.25	600	7.11	10.76	87.94
F13	0	0	1.25	600	7.05	10.79	88.09

Table 9: Summary of ANOVA for response parameters for central composite design for hydrogel

Source	Sum of squares	Degree of freedom	Mean square	F value	P value
pH					
Model	0.26	5	0.051	29.50	0.0001
Residual	0.012	7	1.718E-003	-	-
Corrected Total	0.27	12	-	-	-
Spreadability					
Model	5.96	5	1.19	65.29	0.0001
Residual	0.13	7	0.018	-	-
Corrected Total	6.09	12	-	-	-
Curcumin release					
Model	2.67	2	1.33	4.64	0.0376
Residual	2.88	10	2.67	-	-
Corrected Total	5.55	12	-	-	-

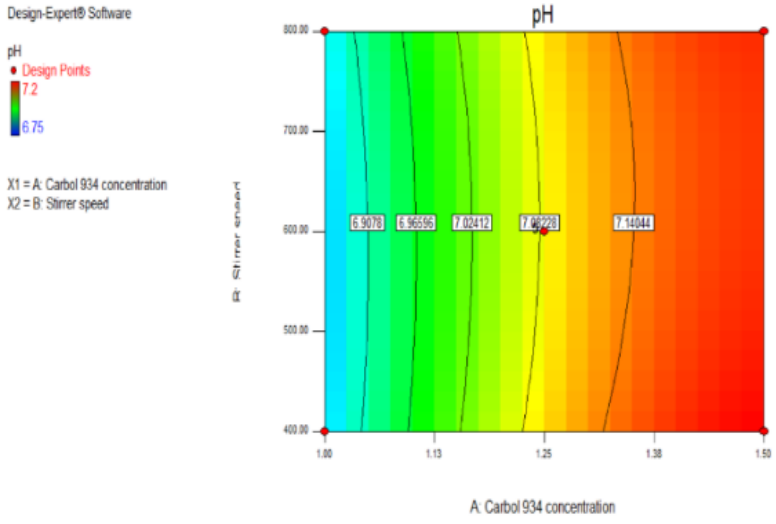

Fig. 9: Contour plot of pH

Effect of factors on pH

Understanding the response surface plot (fig. 10) and its implications for pH optimization, alongside the reduced polynomial equation for pH, is essential for formulating a transferosome system with the desired pH characteristics. The identification of the blue region in both the contour plot (fig. 9) and response surface plot (fig. 10) signifies the optimal area where the pH of the formulation is minimized. This optimal region likely represents conditions that yield the lowest pH values within the experimental range. The high R^2 value of 0.9547 indicates that the model used to predict pH is highly significant. It implies that the model explains a substantial proportion of the variability in the data, strengthening its reliability in predicting pH based on the formulated equation.

Reduced polynomial equation for pH is given below

$$p\text{^}H = 7.09 + 0.16 * A - 0.072A\text{^}2$$

The equation depicts how independent variables influence the response, specifically pH

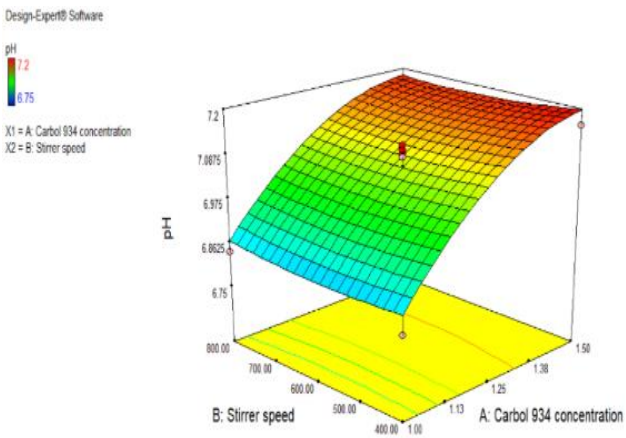

Fig. 10: Response surface plot of ph

Concentration of carbopol

Positive effect: The positive coefficient associated with the concentration of carbopol suggests that increasing the amount of carbopol in the formulation leads to a rise in pH. This indicates that higher concentrations of carbopol contribute to an increase in pH. It is important to manage the carbopol concentration within optimal levels to achieve the desired pH without compromising other aspects of the formulation.

Stirrer speed

Statistically Insignificant: The statement that stirrer speed is statistically insignificant suggests that changes in stirrer speed do not have a significant impact on pH within the studied range. Despite being an independent variable, variations in stirrer speed might not contribute significantly to changes in pH in this specific formulation context.

Effect of factors on spreadability

In the above response surface plot (fig. 12), orange area showed the maximum spreadability. his optimal area likely represents conditions that yield the highest spreadability values within the studied range of parameters. R^2 was found to be 0.9790, which indicates the significance of the model. This suggests that the model explains a substantial portion of the variability in the data, enhancing the reliability of predicting spreadability based on the formulated equation.

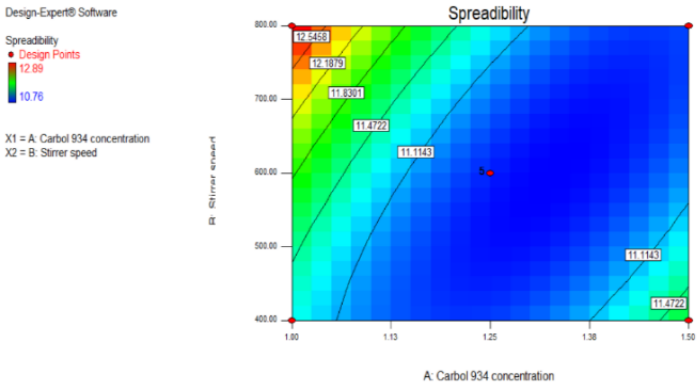

Fig. 11: Contour plot of spreadability

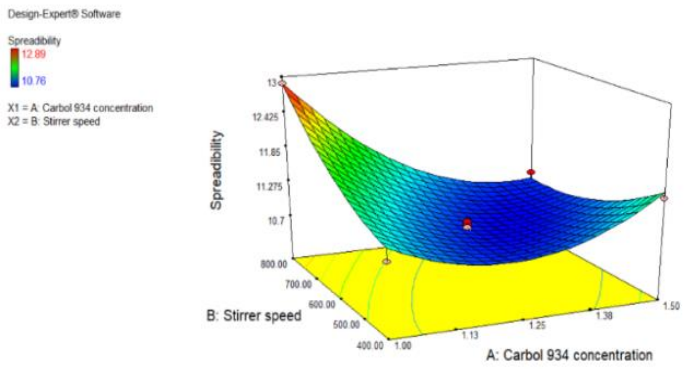

Fig. 12: Response surface plot of spreadability

Reduced polynomial equation for spreadability is given below

$$\text{Spreadability} = +10.83 - 0.42 * A - 0.59 * A * B + 0.62A\text{^}2$$

The equation represents the effect of independent variables on the response i.e., spreadability.

Concentration of carbopol

Positive effect: The positive coefficient associated with the concentration of carbopol suggests that increasing the amount of carbopol in the formulation leads to higher spreadability. This implies that higher concentrations of carbopol positively impact spreadability. Moreover, it indicates a correlation between increased carbopol concentration and higher pH, as Carbopol also affects pH levels.

Stirrer speed

Negative effect: The negative coefficient for stirrer speed indicates that as the stirrer speed increases, the spreadability of the formulation decreases. Higher stirrer speeds seem to have a detrimental effect on the spreadability of the transferosome formulation.

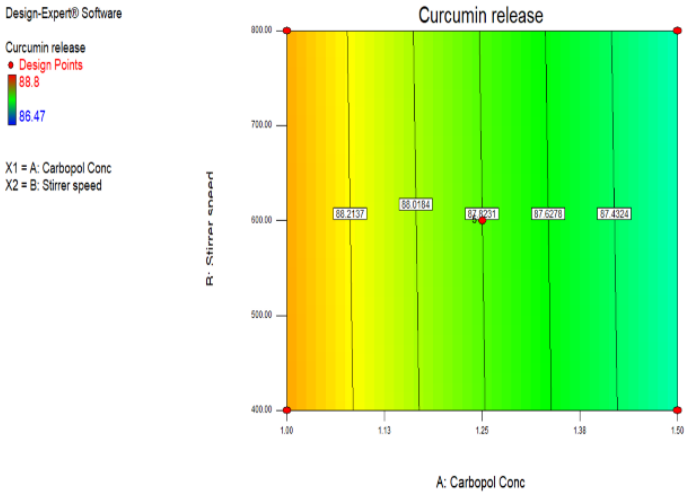

Fig. 13: Contour plot of curcumin release

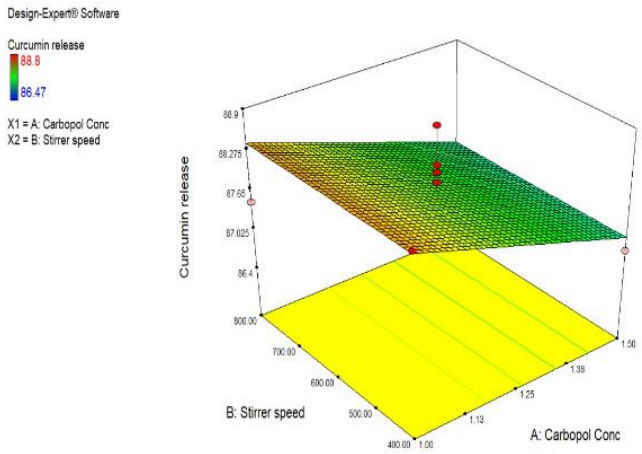

Fig. 14: Response surface plot of curcumin release

Effect of factors on curcumin release

The response surface plot highlighting the yellow area as the region for maximum curcumin release, along with a high coefficient of determination (R^2) of 0.9811, signifies the significance and reliability of the model used for predicting curcumin release based on the formulated equation. The identification of the yellow area in the response surface plot signifies the optimal region where the formulation exhibits maximum curcumin release. This area represents conditions that facilitate the highest release of curcumin from the transferosome system within the studied range of parameters. The high R^2 value of 0.9811 indicates that the model used to predict curcumin release is highly significant. It suggests that the model explains a substantial portion of the variability in the data, highlighting its accuracy and reliability in predicting curcumin release based on the formulated equation.

Reduced polynomial equation for curcumin release is given below

$$\text{Curcumin release} = +87.82 - 0.58 * A - 8.542 - 0.03 * B$$

The above equation illustrates the influence of independent variables on the response, and the release of curcumin. This signifies that the concentration of carbopol exhibits a detrimental impact on curcumin release, resulting in a decrease in curcumin release as the amount of carbopol increases.

Check point method

The result obtained from the performed check point batch was similar to the actual check point batch which was obtained from the D. O. E software without any significant differences.

From the result, after comparing all the parameters with the F3 batch that was similar and no significant differences between

performed, actual, and optimize batch (table 10). So, the close resemblance between the experimental and predicted response value assessed the robustness of the prediction. So F3 batch was selected as the optimized batch out of 13 batches.

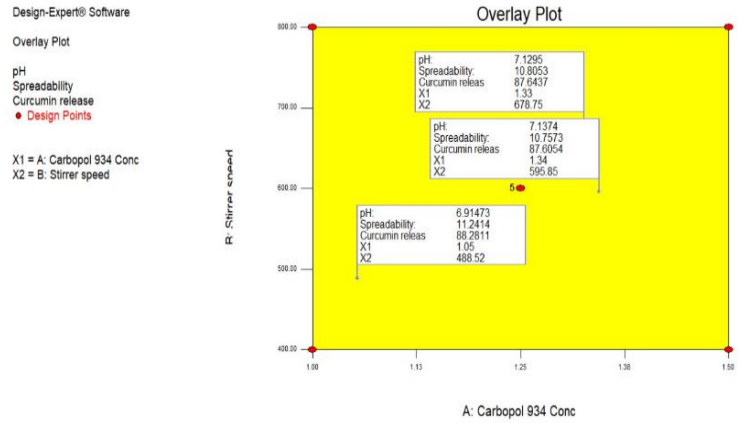

Fig. 15: Overlay plot of pH, spreadability, and curcumin release

Table 10: Comparison of result of performed checkpoint batch (C1, C2, C3 batch) with actual checkpoint batch (A1, A2, A3 batch) and optimized batch (F3 batch)

	Y1: pH	Y2: Spreadability (gm. cm/sec)	Y3: Curcumin release (%)
Performed Check point batch (C1 batch)	7.04	11.68	87.64
Performed Check point batch (C2 batch)	6.86	11.96	87.61
Performed Check point batch (C3 batch)	6.74	11.62	88.28
Actual check point batch (A1 batch)	7.03	11.60	87.60
Actual check point batch (A2 batch)	6.84	11.98	87.59
Actual check point batch (A3 batch)	6.72	11.60	88.25
Optimized batch (F3 batch)	6.84	12.89	87.47

From the analysis (table 10) it was shown that there was no significant difference between actual and performed value on responses Y1. Y2 and Y3. So, the close resemblance between the experimental and predicted response value assessed the robustness of prediction. Thus, F8 batch was selected as optimized batch as transferosome formulation.

***In vitro* drug release**

Diverse kinetic models were employed for the analysis of in vitro release data and the prediction of the mechanism governing drug release. The release constants were derived from the gradients of pertinent plots, while the regression coefficient (R2) was computed. The results indicated that the Higuchi model exhibited the highest linearity, suggesting that it provided the best explanation for the in vitro drug release of the formulation. The regression coefficients (R2) for ascorbic acid, salicylic acid and curcumin were found to be 0.907, 0.9266, and 0.9536, respectively (table 11). These findings suggest that the release of curcumin from the lipid bilayer system primarily occurred through a diffusion mechanism.

Table 11: Comparison of kinetic models

S. No.	Type of release model	$R^2$of curcumin release profile	$R^2$of ascorbic acid release profile	$R^2$of salicylic acid release profile
1	Zero order ($Q_t = Q_0+K0_t$)	0.9617	0.9988	0.9729
2	First order ($\ln Q_t = \ln Q_0+K1t$)	0.6855	0.7592	0.8144
3	Higuchi model ($Q_t = K_H t^{1/2}$)	0.9536	0.907	0.9266
4	korsmeyer-peppas model ($Q_t/Q_8 = Kt^n$)	0.9811	0.8993	0.8708

a **b**

Fig. 16: Skin irritancy study by using Albino a) Control rat skin b) Skin treated with hydrogel

***In vivo* studies (Skin irritation studies)**

The formulation was subjected to a skin irritation test *in vivo*, evaluating the scores for erythema and edema which is shown in fig. 16 (a) and (b). After applying the formulation, no visible indications of erythema, edema, or inflammation were detected on the skin. Conversely, the formalin solution led to notable skin irritation [32]. These findings indicate that the developed transdermal formulation does not cause skin irritation and can be considered non-irritating.

Drug content

The optimized batch F3 showed pH of 6.84, spreadability of 12.89 gm. cm/sec and curcumin release of 87.47%. The optimized batch exhibited drug contents of 99.25±0.07% for curcumin, 98.76±0.38% for ascorbic acid, and 97.28±0.35% for salicylic acid.

CONCLUSION

It can be concluded that the application of experimental design is helpful tool for the development of curcumin transferosomes as nanobiocomposite formulation. During the preliminary studies, it was found that the there are various factors that affect the preparation of transferosomes**.** Using Design-Expert v7.0.0 software, a 3^2 full factorial design was utilized as an optimization technique to determine the key factors influencing the formulation of transferosomes. In this study amount of edge activator and sonication time plays and important role for the preparation of Transferosomes. From the screening study, formulation containing Phospholipon 90G have good entrapment efficiency and vesicle size compare to Phospholipon 90H. The developed curcumin-loaded hydrogel yielded stable, nano-sized vesicles characterized by elevated encapsulation efficiency and a diminutive particle size. Furthermore, the preparation of curcumin as a transferosome gel demonstrated the capability to overcome skin barrier properties, resulting in increased drug release. Honey was incorporated to enhance the tensile strength of hydrogel, which has also been proven effective as a wound-healing agent. It is safe for wound healing because there is no skin irritation.

FUNDING

Nil

AUTHORS CONTRIBUTIONS

All the authors have contributed equally.

CONFLICT OF INTERESTS

The authors have no conflicts of interest regarding this investigation.

REFERENCES

1. Ramya Devi D, Sowmiya Lakshna S, Veena Parvathi S, Vedha Hari BN. Investigation of wound healing effect of topical gel of Albizia amara leaves extract. S Afr J Bot. 2018;119:400-9. doi: 10.1016/j.sajb.2018.10.005.
2. Bachmeier BE, Melchart D. Therapeutic effects of curcumin-from traditional past to present and future clinical applications. Int J Mol Sci. 2019;20(15):3757-60. doi: 10.3390/ijms20153757, PMID 31374813.
3. https://www.cancer.gov/publications/dictionaries/cancer-drug/def/ascorbic-acid.
4. Akram MW, Jamshaid H, Rehman FU, Zaeem M, Khan JZ, Zeb A. Transfersomes: a revolutionary nanosystem for efficient transdermal drug delivery. AAPS PharmSciTech. 2021;23(1):7. doi: 10.1208/s12249-021-02166-9, PMID 34853906.
5. Patel R, Singh SK, Singh S, Sheth NR, Gendle R. Development and characterization of curcumin loaded transferosome for transdermal delivery. J Pharm Sci Res. 2009;1(4):71-80.
6. Sharma M. Transdermal and intravenous nano drug delivery systems: present and future. In: Applications of targeted nano drugs and delivery systems. Elsevier. 2019;18(1):499-550. doi: 10.1016/B978-0-12-814029-1.00018-1.
7. Ogihara Umeda I, Sasaki T, Toyama H, Oda K, Senda M, Nishigori H. Rapid diagnostic imaging of cancer using radiolabeled liposomes. Cancer Detect Prev. 1997;21(6):490-6. PMID 9398989.
8. Ahmad I, Ali Sheraz M, Ahmed S, Shad Z, Vaid FH. Photostabilization of ascorbic acid with citric acid, tartaric acid and boric acid in cream formulations. Int J Cosmet Sci. 2012;34(3):240-5. doi: 10.1111/j.1468-2494.2012.00708.x, PMID 22296174.
9. Gupta T, Singh J, Kaur S, Sandhu S, Singh G, Kaur IP. Enhancing bioavailability and stability of curcumin using solid lipid nanoparticles (CLEN): a covenant for its effectiveness. Front Bioeng Biotechnol. 2020;8:879. doi: 10.3389/fbioe.2020.00879, PMID 33178666.
10. Boateng JS, Matthews KH, Stevens HN, Eccleston GM. Wound healing dressings and drug delivery systems: a review. J Pharm Sci. 2008;97(8):2892-923. doi: 10.1002/jps.21210, PMID 17963217.
11. Strodtbeck F. Physiology of wound healing. Newborn Infant Nurs Rev. 2001;1(1):43-52. doi: 10.1053/nbin.2001.23176.
12. Tatsioni A, Balk E, O'Donnell T, Lau J. Usual care in the management of chronic wounds: a review of the recent literature. J Am Coll Surg. 2007 Oct 1;205(4):617-624e57. doi: 10.1016/j.jamcollsurg.2007.05.032, PMID 17903739.
13. Tatsioni A, Balk E, O'Donnell T, Lau J. Usual care in the management of chronic wounds: a review of the recent literature. J Am Coll Surg. 2007;205(4):617-624e57. doi: 10.1016/j.jamcollsurg.2007.05.032, PMID 17903739.
14. Shetty T, Dubey A, Ravi GS, Hebbar S, Shastry CS, Charyulu N. Antifungal and antioxidant therapy for the treatment of fungal infection with microemulsion gel containing curcumin and vitamin C. Asian J Pharm. 2017 Oct 1;11(1):17-725:10.22377/ajp.v11i04.1700.
15. Vasanth S, Dubey A, GSR, Lewis SA, Ghate VM, El-Zahaby SA. Development and investigation of vitamin C-enriched adapalene-loaded transfersome gel: a collegial approach for the treatment of acne vulgaris. AAPS PharmSciTech. 2020;21(2):61. doi: 10.1208/s12249-019-1518-5, PMID 31915948.
16. Arora R, Aggarwal G, Dhingra GA, Nagpal M. Herbal active ingredients used in skin cosmetics. Asian J Pharm Clin Res. 2019;12(9):7-15. doi: 10.22159/ajpcr.
17. Patel NA, Patel NJ, Patel RP. Formulation and evaluation of curcumin gel for topical application. Pharm Dev Technol. 2009;14(1):80-9. doi: 10.1080/10837450802409438, PMID 18821270.
18. Sahu JP, Khan AI, Maurya R, Shukla AK. Formulation development and evaluation of transferosomal drug delivery for effective treatment of acne. A Astrophysical Journal. 2019;4(1):26-34. doi: 10.31024/APJ.2019.4.1.4C.
19. Thakur N, Jain P, Jain V. Formulation development and evaluation of transferosomal gel. J Drug Delivery Ther. 2018;8(5):168-77. doi: 10.22270/jddt.v8i5.1826.
20. Gayathri H, Sangeetha S. Pharmaceutical development of tamoxifen citrate loaded transferosomal gel for skin cancer by design of experiments (DoE) approach. J Pharm Neg Results. 2022;13(5):2456-68.
21. OECD. Acute Dermal Irritation/Corrosion, OECD Guidelines for the Testing of Chemicals, Section 4. Paris: OECD Publishing; 2015. doi: 10.1787/9789264242678-en.
22. Shukla SK, Sharma AK, Gupta V, Yashavarddhan MH. Pharmacological control of inflammation in wound healing. J Tissue Viability. 2019 Nov;28(4):218-22. doi: 10.1016/j.jtv.2019.09.002, PMID 31542301.
23. Sajjadi P, Khodayar MJ, Sharif Makhmalzadeh BS, Rezaee S. Percutaneous absorption of salicylic Acid after administration of trolamine salicylate cream in rats with transcutol(®) and eucalyptus oil pre-treated skin. Adv Pharm Bull. 2013;3(2):295-301. doi: 10.5681/apb.2013.048, PMID 24312851.
24. Mullassery MD, Fernandez NB, RS, Thomas D. A green approach for the synthesis of drug delivery system, mesoporous silica grafted acrylamide –β- cyclodextrin composite, for the controlled release of curcumin. Asian J Pharm Clin Res. 2018;11(9). doi: 10.22159/ajpcr.2018.v11i9.26769.
25. Bh, NR, Ranjan Rauta VV, S Sreenivasa. "Synthesis and characterization of novel SaA-Ppa-Lsa/C-30b/Ag nanocomposites for swelling, antibacterial, drug delivery, and anticancer applications". AJPCR. 2018;11(3):329-38. 10.22159/ajpcr.2018.v11i3.22939.

26. Maiti K, Mukherjee K, Gantait A, Saha BP, Mukherjee PK. Curcumin-phospholipid complex: preparation, therapeutic evaluation and pharmacokinetic study in rats. Int J Pharm. 2007 Feb 7;330(1-2):155-63. doi: 10.1016/j.ijpharm.2006.09.025, PMID 17112692.
27. Du Lina, Feng Xue, Xiang Xiaoqin, Jin Yiguang. Wound healing effect of an in situ forming hydrogel loading curcumin-phospholipid complex. Curr Drug Deliv. 2016;13(1):76-82. doi: 10.2174/1567201813666151202195437, PMID 26634789.
28. Omar MM, Hasan OA, El Sisi AM. Preparation and optimization of lidocaine transferosomal gel containing permeation enhancers: a promising approach for enhancement of skin permeation. Int J Nanomedicine. 2019;14:1551-62. doi: 10.2147/IJN.S201356, PMID 30880964.
29. Iskandarsyah Iskandarsyah, Masrijal Camelia Camelia Dwi Putri, Harmita Harmita. Effects of sonication on size distribution and entrapment of lynestrenol transferosome. Int J App Pharm. 2020;FF053:245-7. doi: 10.22159/ijap.2020.v12s1.FF053.
30. Opatha SAT, Titapiwatanakun V, Chutoprapat R. Transfersomes: a promising nanoencapsulation technique for transdermal drug delivery. Pharmaceutics. 2020 Sep 9;12(9):855.10.3390. doi: 10.3390/pharmaceutics12090855, PMID 32916782.
31. Kumar A, Kurmi BD, Singh D. Development and method validation of design of experiments-optimized tablet formulation for simultaneous detection of exemestane and everolimus. Assay Drug Dev Technol. 2023 Aug-Sep;21(6):273-87. doi: 10.1089/adt.2023.055, PMID 37682343.
32. Kumar B, Aggarwal R, Prakash U, Sahoo PK. Emerging therapeutic potential of curcumin in the management of dermatological diseases: an extensive review of drug and pharmacological activities. Futur J Pharm Sci. 2023 May;9(1). doi: 10.1186/s43094-023-00493-1.